Three-photon spectroscopy of excitons and polaritons in alkali halides

F. Beerwerth, D. Fröhlich, P. Köhler, V. Leinweber, and A. Voss
Institut für Physik, Universität Dortmund, 4600 Dortmund 50, Federal Republic of Germany
(Received 5 February 1988)

Three-photon spectra of nine alkali halides are presented. The nonlinear-optical method of three-photon spectroscopy allows one to measure resonances on the upper polariton branch and the longitudinal exciton at different values of the total k vector. The analysis of the polariton dispersion yields reliable values of the longitudinal-transverse splitting. In Cs halides new exciton lines of Γ_5^- symmetry are resolved which are forbidden for one-photon optical transitions. In high magnetic fields transitions to paraexcitons of Γ_5^- and Γ_3^- symmetry are allowed. The g values for the uppermost valence band and the lowest conduction band are derived from the Zeeman splitting of the paraexcitons and the transverse polariton. In addition, the exchange energy for KI and RbI is gained from the three-photon spectra in high magnetic fields.

I. INTRODUCTION

Nonlinear-optical methods have gained increasing interest as a powerful tool for the investigation of electronic parameters of semiconductors and insulators. Because of additional degrees of freedom in the experiments, where more than one photon is participating in an elementary absorption process, one expects additional information as compared to the classical one-photon absorption (OPA). Two-photon absorption (TPA) is a good example to demonstrate this point. There are two interesting aspects if one compares OPA and TPA. (i) Due to different selection rules new exciton lines can be seen in TPA which are dipole forbidden in OPA. Even-parity excitons in Cu_2O (Ref. 1) (S and D excitons) and P excitons in II-VI and III-V compounds as ZnSe,[2] CdTe,[3] and GaAs (Ref. 4) are well resolved in TPA. High-resolution experiments in magnetic fields yield reliable data of electronic parameters. Complications due to degenerate valence bands[4] have to be taken into account. (ii) k-space spectroscopy is considered as a second interesting aspect of TPA. The fact that in TPA it is possible to change the total energy ($\hbar\omega=\hbar\omega_1+\hbar\omega_2$) and the total k vector ($\mathbf{k}=\mathbf{k}_1+\mathbf{k}_2$) within certain limitations independently of each other allows one to excite resonances on the upper polariton branch and even on the longitudinal exciton branch. k-space spectroscopy of a polariton structure by TPA is limited to crystals without an inversion center, since the relevant optical transition has to be simultaneously allowed for OPA and TPA. As an example we mention measurements of the exciton-polariton structure in CuCl (Ref. 5) and $AgGaS_2$.[6] The limitation of k-space spectroscopy to crystals without inversion symmetry in TPA was the main motivation to move on to three-photon spectroscopy (TPS). The dipole selection rules show that all transitions which are allowed in OPA are also allowed in TPS. It should thus be possible to measure the polariton structure in systems with inversion symmetry. Beerwerth and Fröhlich[7] have recently presented first measurements of the polariton structure of alkali iodides gained by TPS. The other aspect of nonlinear spectroscopy, that additional transitions are allowed as compared to linear spectroscopy, is considered in further TPS experiments by Beerwerth and Fröhlich.[8,9] New very narrow exciton lines of Γ_5^- and Γ_3^- symmetry, which are forbidden in OPA, are detected in CsI and KI by TPS. Measurements of these narrow lines in high magnetic fields yield information on important electronic parameters like g values and exchange energies.

In this paper we present three-photon spectra of many more alkali halides. We have succeeded in measuring spectra of alkali iodides (NaI, KI, RbI, CsI), alkali bromides (NaBr, KBr, RbBr, CsBr), and even one alkali chloride (NaCl). In some of these substances we have measured the polariton structure in detail (KI, RbI, CsI). The polariton structure in CsI is quite complicated, since there are three close-lying excitons. From the experimental data we derive values for the longitudinal excitons and the longitudinal-transverse splitting. For KI, RbI, and CsI we present measurements in high magnetic fields (up to 9 T). The analysis of the three-photon magnetoabsorption data yields accurate g values and the important exchange parameter for KI and RbI.

The paper is organized as follows. In the next section we discuss details of the exciton structure in alkali halides. We limit our discussion to transitions from the uppermost valence band to the lowest conduction bands. After a short section on the experimental setup we present our experimental data and a discussion.

II. EXCITONS IN ALKALI HALIDES

Excitonic transitions in alkali halides were first observed by Hilsch and Pohl[10] more than 50 years ago. About 20 years later Martienssen[11] investigated further details of the excitons in alkali halides including their temperature dependence. The most detailed study of excitons in alkali halides was made by Teegarden and Baldini.[12] We refer to their spectra for comparison with our three-photon results. Since we are only interested in the

lowest excitons, we restrict our discussion of the band structure to the upper valence bands and the lower conduction bands. For a detailed discussion of different exciton models in alkali halides we refer to the book by Knox.[13] We analyze the exciton states on the basis of the energy-band picture. Taking spin-orbit coupling into account one derives from halogen p states an uppermost valence band of Γ_8^- ($j_v=\frac{3}{2}$) and a lower valence band of Γ_6^- ($j_v=\frac{1}{2}$) symmetry. The lowest conduction band is derived from alkali s states which lead to a band of Γ_6^+ ($j_c=\frac{1}{2}$) symmetry. For band calculations and further literature we refer to publications by Kunz.[14] In CsCl-type alkali halides as CsI, CsBr, and CsCl (not CsF) there is a second low-lying conduction band, which is due to alkali d states. Including spin this band is of Γ_8^+ ($j_c=\frac{3}{2}$) symmetry. A detailed discussion of the energy bands in Cs halides is given by Onodera.[15] Since we consider only S excitons, the symmetry of the excitons can be directly derived from the coupling of the appropriate valence- and conduction-band j values to a total angular momentum F. For $j_v=\frac{3}{2}$ (Γ_8^-) and $j_c=\frac{1}{2}$ (Γ_6^+) we get $F=2$ (Γ_3^-,Γ_5^-) and $F=1$ (Γ_4^-). The $\Gamma_i^{\pm}$ in parentheses refer to the quantum numbers in cubic symmetry, which are derived with the use of the tables of Koster *et al.*[16] The $F=2$ state is a pure triplet state (paraexciton), which is dipole forbidden. The $F=1$ state (orthoexciton) is a singlet-triplet mixed state and dipole allowed. Due to the strong coupling of the $F=1$ state to the electromagnetic field we get new eigenstates of the coupled system. The resulting polariton dispersion consists of an upper and a lower polariton branch and a longitudinal exciton branch. The $F=1$ and $F=2$ states are split by the exchange interaction as discussed in detail by Onodera and Toyozawa.[17] Following their notation the analytic exchange energy is defined as

$$\Delta_{ex}=\tfrac{3}{2}(E_T-E_P)=\tfrac{3}{2}(E_L-\Delta_{LT}-E_P)\ , \tag{1}$$

where E_L, E_T, and E_P denote the energy values of the transverse, longitudinal, and paraexciton, respectively. Δ_{LT} is the longitudinal-transverse splitting (nonanalytic exchange interaction).

In Cs halides we have an additional $j_c=\frac{3}{2}$ (Γ_8^+) band, which has again to be coupled to the uppermost valence band ($j_v=\frac{3}{2}$). This coupling leads to the following states with total angular momentum: $F=3$ ($\Gamma_2^-,\Gamma_4^-,\Gamma_5^-$), $F=2$ (Γ_3^-,Γ_5^-), $F=1$ (Γ_4^-), and $F=0$ (Γ_1^-). From this decomposition one would expect only one dipole active transition to the $F=1$ state in addition to the $F=1$ state from the s-like conduction band (Γ_6^+). In the one-photon spectra, however, one observes three strong exciton lines. The third resonance corresponds to a transition to the Γ_4^- component of the $F=3$ state, which gets allowed by Coulomb interaction. This point is discussed in detail by Iwamoto and Onaka.[18]

In TPS many more states are dipole allowed as compared to only $F=1$ states in OPA. With the use of the tables of Koster *et al.*[16] one finds out that all 16 states ($\Gamma_1^-,\Gamma_2^-,\Gamma_3^-,2\Gamma_4^-,2\Gamma_5^-$) of the $j_v=\frac{3}{2}$ to $j_c=\frac{3}{2}$ transition are allowed if one applies three times the dipole operator of Γ_4^- symmetry starting from the totally symmetric state of Γ_1^+ symmetry. In a second step one has to investigate, which of these states belong to pure triplet states (paraexcitons), since three-photon transitions to paraexcitons are spin forbidden. In order to find out which of the states contain singlet contributions (orthoexcitons) one derives the exciton quantum numbers in the LS-coupling scheme. The analysis shows that there is an additional Γ_5^- orthoexciton, which can be excited by TPS. A second Γ_5^- exciton might get allowed again by Coulomb interaction as discussed for the Γ_4^- excitons in OPA. Indeed in CsI we find two more exciton lines in TPS as compared to OPA, which we assign to Γ_5^- excitons.

Since the lowest of these new exciton lines exhibits an extremely small linewidth (0.15 meV) compared to the Γ_4^- excitons (10 meV), the Zeeman splitting can easily be resolved as shown by Beerwerth and Fröhlich.[8] In addition to a splitting of degenerate exciton states one gets a mixing of ortho- and parexcitons in high magnetic fields. By this mixing paraexcitons gain oscillator strength from the orthoexcitons and should therefore be observable. The $F=2$ (Γ_5^-,Γ_3^-) paraexciton was recently seen.[9] In the following we will briefly discuss the field-induced mixing and splitting of an $F=1$ orthoexciton and an $F=2$ paraexciton for a magnetic field in a [001] direction. The analysis is directly applicable to our experimental results of KI and RbI which are presented in the last chapter. In Fig. 1 we present a schematic level diagram of the ortho-para-exciton structure as a function of an external magnetic field. Besides the longitudinal-transverse splitting Δ_{LT} and the analytic exchange Δ_{ex} we have introduced a small splitting ε_{ex} between the Γ_5^- and Γ_3^- states due to anisotropic exchange.[19] Our experiments show that ε_{ex} is about 0.1 meV. For magnetic fields $B>2$ T we can neglect this splitting. The spherical quantum numbers can then also be used for the $M=\pm2$ components, since we get a complete mixture of the Γ_{32}^- and Γ_{50}^- states [$|M=\pm2\rangle=(1/\sqrt{2})(|\Gamma_{32}^-\rangle\pm|\Gamma_{50}^-\rangle)$]. Defining the g

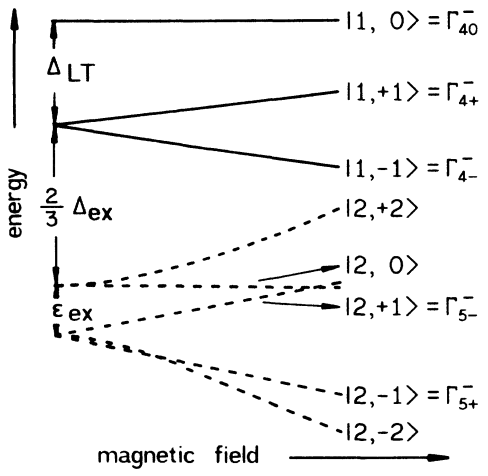

FIG. 1. Schematic level diagram of the orthoexciton ($F=1$) and paraexciton ($F=2$) as a function of magnetic field.

TABLE I. Matrix of the Zeeman operator H_Z and exchange interaction corresponding to schematic level diagram of Fig. 1. g values and exchange parameters are defined in the text.

		$F=1$				$F=2$		
	$\lvert\Gamma_{4+}^{-}\rangle$	$\lvert\Gamma_{40}^{-}\rangle$	$\lvert\Gamma_{4-}^{-}\rangle$	$\lvert\Gamma_{31}^{-}\rangle$	$\lvert\Gamma_{32}^{-}\rangle$	$\lvert\Gamma_{5+}^{-}\rangle$	$\lvert\Gamma_{50}^{-}\rangle$	$\lvert\Gamma_{5-}^{-}\rangle$
$\lvert\Gamma_{4+}^{-}\rangle$	$\frac{2}{3}\Delta_{ex}+g_o\mu_B B$	0	0	0	0	0	0	$\sqrt{3}g_{op}\mu_B B$
$\lvert\Gamma_{40}^{-}\rangle$	0	$\frac{2}{3}\Delta_{ex}+\Delta_{LT}$	0	$-ig_{op}\mu_B B$	0	0	0	0
$\lvert\Gamma_{4-}^{-}\rangle$	0	0	$\frac{2}{3}\Delta_{ex}-g_o\mu_B B$	0	0	$\sqrt{3}g_{op}\mu_B B$	0	0
$\lvert\Gamma_{31}^{-}\rangle$	0	$ig_{op}\mu_B B$	0	ε_{ex}	0	0	0	0
$\lvert\Gamma_{32}^{-}\rangle$	0	0	0	0	ε_{ex}	0	$-i2g_p\mu_B B$	0
$\lvert\Gamma_{5+}^{-}\rangle$	0	0	$\sqrt{3}g_{op}\mu_B B$	0	0	$-g_p\mu_B B$	0	0
$\lvert\Gamma_{50}^{-}\rangle$	0	0	0	0	$i2g_p\mu_B B$	0	0	0
$\lvert\Gamma_{5-}^{-}\rangle$	$\sqrt{3}g_{op}\mu_B B$	0	0	0	0	0	0	$g_p\mu_B B$

values for electron and hole as g_c and g_v, respectively, we get for the Zeeman operator

$$H_Z=\mu_B B(g_c j_{cz}+g_v j_{vz}) , \tag{2}$$

where **B** is oriented along a [001] crystalline direction. μ_B stands for the Bohr magneton, and j_{cz} and j_{vz} are the z components of quasispin operators for electron and hole, respectively. The matrix elements in Table I are calculated with the use of the tables of Koster *et al.*[16] The matrix contains three effective g values. The $F=1$ ($M\pm1$) orthoexciton is split proportional to $g_o=\frac{1}{4}(5g_v-g_c)$. The exciton resonances are given by

$$E(F=1,M=\pm1)=E_P+\tfrac{2}{3}\Delta_{ex}\pm g_o\mu_B B . \tag{3}$$

Δ_{ex} denotes the analytic exchange energy as defined by Eq. (1). The mixing of the $F=1$ orthoexciton and $F=2$ paraexciton is due to the off-diagonal g value $g_{op}=\frac{1}{2}(g_v-g_c)$. A small repulsion of the $F=1$ and $F=2$ states by this mixing is neglected. The splitting of the $F=2$ state is determined by $g_p=\frac{1}{4}(3g_v+g_c)$. For the field dependence of the paraexciton components we get

$$E_P(M=\pm1)=E_P\pm g_p\mu_B B , \tag{4}$$

$$E_P(M=\pm2)=E_P+\varepsilon_{ex}/2\pm[(2g_p\mu_B B)^2+(\varepsilon_{ex}/2)^2]^{1/2}$$
$$\approx E_P+\varepsilon_{ex}/2\pm\left[2g_p\mu_B B+\frac{\varepsilon_{ex}^2}{16g_p\mu_B B}\right] . \tag{5}$$

The experimental results show that the correction term $\varepsilon_{ex}^2/16g_p\mu_B B$ can be neglected already for rather low fields ($B\sim2$ T).

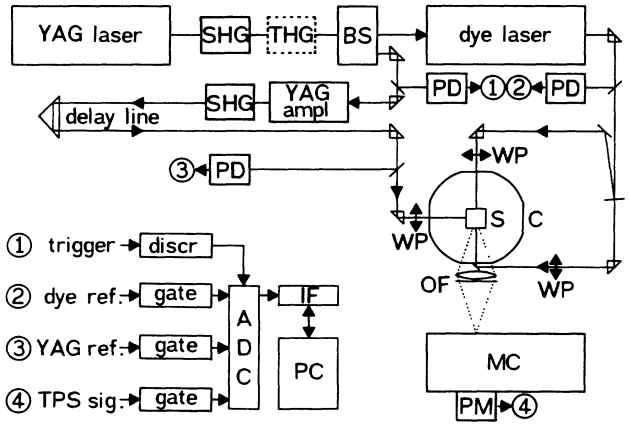

FIG. 2. Experimental setup for three-photon spectroscopy. SHG/THG, second- and third-harmonic generator; BS, beam separator; PD, photodiode; WP, quarter- or half-wave plate; S, sample; C, cryostat; OF, optical filter; MC, monochromator; PM, photomultiplier, discr., discriminator; IF, computer interface; PC, on-line calculator; and ADC, analog to digital converter.

III. EXPERIMENTAL SETUP

For our experiments we used ultrapure single crystals. Besides the Cs halides all crystals were cleaved in a dry atmosphere before they were mounted in a cryostat. The sizes of the crystals range from 2 to 10 mm. NaI had to be handled in an extremely dry atmosphere (dew point about -20 °C), because it is very hygroscopic. The Cs halides were oriented by use of stress-induced birefringence as described by Maier.[20] These crystals were cut, polished, and carefully annealed. Most of the measurements were done in an immersion cryostat at a temperature of about 1.5 K. The magnetic fields for the

TABLE II. Luminescence lines as used in TPS experiments. For literature we refer to Itoh (Ref. 21).

Substance	λ (nm)
NaI	295
KI	300
RbI	315
CsI	288,325
NaBr	267
KBr	282
RbBr	299
CsBr	269,343
NaCl	230

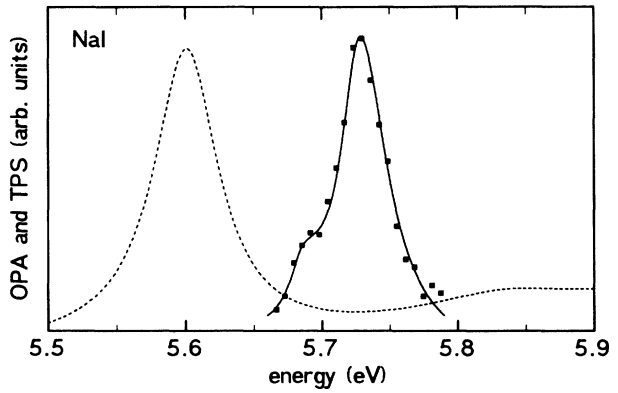

FIG. 3. Three-photon spectrum of NaI at 1.5 K. One-photon absorption (dashed line) from Ref. 12.

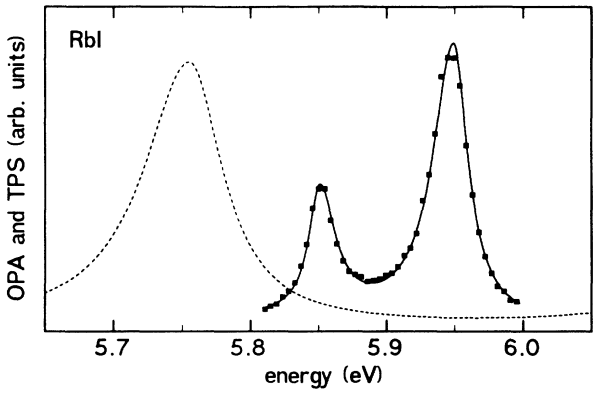

FIG. 5. Three-photon spectrum of RbI at 1.5 K. One-photon absorption (dashed line) from Ref. 12.

measurements in Faraday and Voigt configuration were produced by a superconducting magnet at 4.2 K or at about 2 K: fields up to 9 T were available. For the B field measurements the samples were cooled by exchange gas (He).

The experimental setup is shown schematically in Fig. 2. As a light source we used a frequency-doubled or frequency-tripled Nd-doped yttrium-aluminum-garnet laser (Quanta Ray DCR-2A) to pump a tunable dye laser (Lambda Physik FL2002). The spectral resolution of the system was better than 50 μeV. For the detailed measurements of the k-dependent resonances it was much more favorable to use one photon of the pump laser (532 nm) and two photons of the tunable dye-laser beam (665–695 nm for CsI); the latter was split into two beams before being focused onto the sample. The maximum light intensity of the dye laser was about 200 MW/cm^2, whereas the fixed-frequency laser was kept below 50 MW/cm^2 in order to suppress three-photon transitions of this laser alone to continuum states, which then result in a background signal. With the use of different geometrical configurations for the three laser beams, we were able to excite resonances between $0.22k_{\max}$ and $k_{\max}$. In the $k_{\max}$ configuration all beams are parallel.

For the excitation of the longitudinal exciton (LE) one has to choose an appropriate polarization and k vector configuration. The final Γ_4^- state, which is excited by the three incoming photons, has to have a component parallel to the total k vector ($\mathbf{k}=\mathbf{k}_1+\mathbf{k}_2+\mathbf{k}_3$). An equivalent case is discussed in detail by Fröhlich, Mohler, and Uihlein[5] for two-photon absorption (TPA) in CuCl. Replacing the TPA-polarization dependence to a Γ_5 state by the TPS-polarization dependence to a Γ_4^- state we can proceed as in Ref. 5. The polar vector $\mathbf{b}$, which determines the direction of the nonlinear polarization of the final $F=1$ (Γ_4^-) state, can easily be calculated in a spherical approximation by applying the dipole operator three times ($\Delta F=\pm 1$). We get

$$\mathbf{b}=\epsilon_1(\epsilon_2\cdot\epsilon_3)+\epsilon_2(\epsilon_3\cdot\epsilon_1)+\epsilon_3(\epsilon_1\cdot\epsilon_2)\ , \tag{6}$$

where ϵ_1, ϵ_2, and ϵ_3 are the polarization vectors of the incoming photon beams. Introducing $\mathbf{s}=\mathbf{k}/|\mathbf{k}|$ as a unit

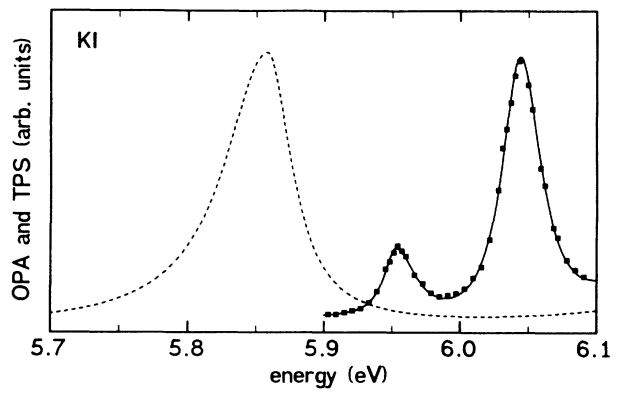

FIG. 4. Three-photon spectrum of KI at 1.5 K. One-photon absorption (dashed line) from Ref. 12.

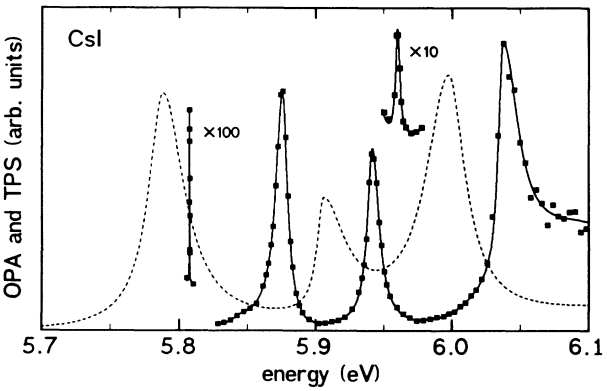

FIG. 6. Three-photon spectrum of CsI at 1.5 K. Weak lines at 5.8076 and 5.960 eV are measured with circularly polarized light. One-photon absorption (dashed line) from Ref. 12.

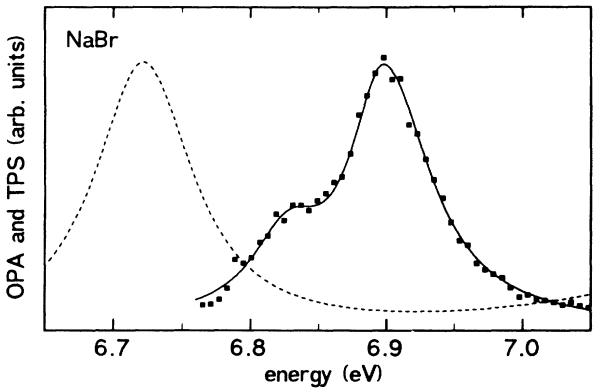

FIG. 7. Three-photon spectrum of NaBr at 1.5 K. One-photon absorption (dashed line) from Ref. 12.

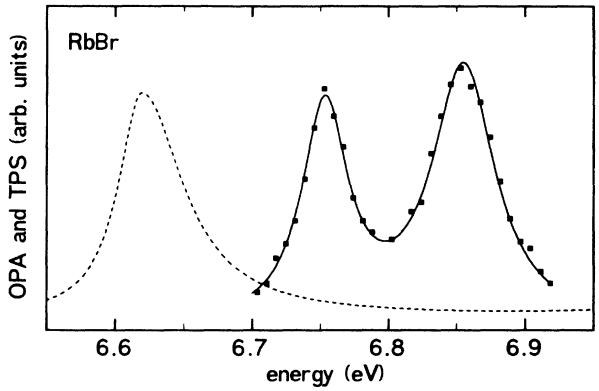

FIG. 9. Three-photon spectrum of RbBr at 1.5 K. One-photon absorption (dashed line) from Ref. 12.

vector pointing in the direction of the total k vector, the oscillator strength f_{LE} for the LE is given by

$$f_{\mathrm{LE}}=f_0(\omega_{\mathrm{LE}})(\mathbf{s}\cdot\mathbf{b})^2 \ . \tag{7}$$

$f_0(\omega_{\mathrm{LE}})$ is a factor, which does not depend on the polarization vectors and the direction of the total k vector. For the excitation of the transverse polariton (TP), one has to consider the component of **b**, which is perpendicular to **s**:

$$f_{\mathrm{TP}}=f_0(\omega_{\mathrm{TP}})(\mathbf{s}\times\mathbf{b})^2 \ . \tag{8}$$

The three-photon absorption was detected via the luminescence of the self-trapped exciton. It is advantageous to use the luminescence lines at high photon energies in order to get a sufficient suppression of background signals, which might be induced by two-photon processes. The luminescence pulse was separated from the strong exciting laser pulses by a prism monochromator (Zeiss M 4 Q III) and appropriate filters. For the detection of the very weak paraexciton resonances in KI and RbI we finally succeeded in measuring about one photon in the detection channel, when about 10^{16} photons of a 5-ns laser pulse were focused onto the crystal. The luminescence lines for the different substances are given in Table II. The optical signals were detected by a photomultiplier and normalized to the intensities of the laser beams. The electronic signals were digitized and averaged over 20–100 pulses by an on-line calculator. The calculator also controlled the wavelength setting of the dye laser and the setting of the polarizing optics (half- and quarter-wave plates). The whole setup can be considered an automatic three-photon spectrophotometer. A typical spectrum is measured in about 20 min.

IV. EXPERIMENTAL RESULTS AND DISCUSSION

This section is divided into three parts. In the first part we show our three-photon spectra of all nine alkali halides measured up to now. The second part is devoted to the detailed polariton structure of RbI and CsI. In the last part we present three-photon magnetooptic data of the para- and orthoexciton in RbI and a new Γ_5^- exciton in CsI.

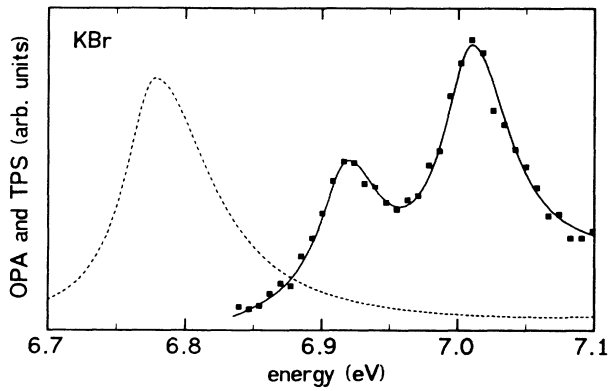

FIG. 8. Three-photon spectrum of KBr at 1.5 K. One-photon absorption (dashed line) from Ref. 12.

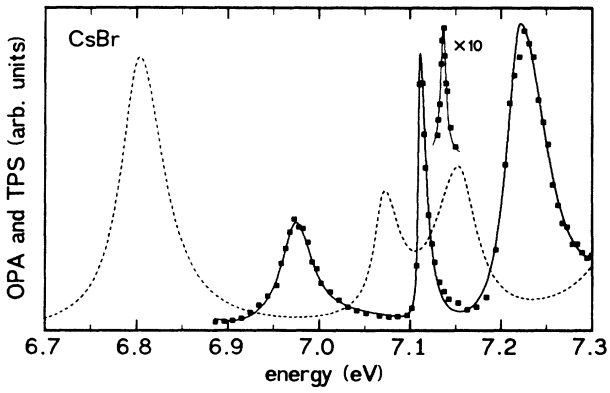

FIG. 10. Three-photon spectrum of CsBr at 1.5 K. Weak line at 7.136 eV is measured with circularly polarized light. One-photon absorption (dashed line) from Ref. 12.

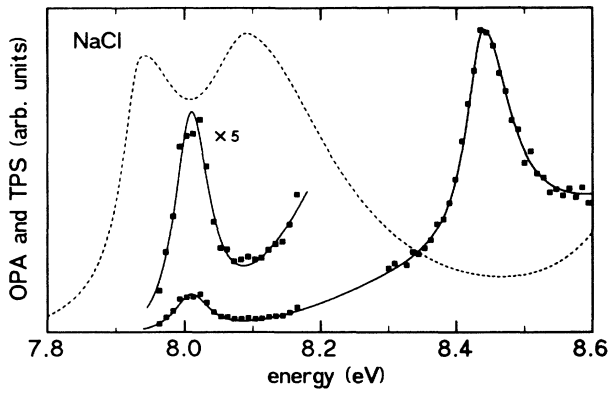

FIG. 11. Three-photon spectrum of NaCl at 1.5 K. One-photon absorption (dashed line) from Ref. 12.

In Figs. 3–11 three-photon spectra of nine alkali halides are shown together with the one-photon spectra of Teegarden and Baldini.[12] All spectra are measured with only one laser beam. The high-energy peak corresponds to the k_{max} resonance on the upper polariton branch. The weaker second peak on the low-energy side in NaI, KI, RbI, NaBr, KBr, and RbBr corresponds to the polariton resonance at $\frac{1}{3}k_{max}$ which is caused by a reflection of the incoming laser beam at the back face of the crystal. The energy difference between these two resonances at k_{max} and $\frac{1}{3}k_{max}$ is a direct measure of the polariton dispersion. In CsI and CsBr special care was taken to suppress the $\frac{1}{3}k_{max}$ resonance by crystal preparation. Due to the additional conduction band (Γ_8^+ symmetry) one gets in the Cs halides three Γ_4^- polaritons. In CsI (Fig. 6) we found two more resonances, which we assign to Γ_5^- excitons as discussed in the Sec. II. The very narrow Γ_5^- line at 5.8076 eV was studied in detail by three-photon magnetoabsorption.[8] The new rather weak line at 5.960 eV could only be seen with circularly polarized light. The use of circular polarization was necessary in order to suppress the adjacent strong $F=1$ (Γ_4^-) line sufficiently. The assignment of this line to a Γ_5^- exciton is supported by measurements in high magnetic fields (8 T). The line shows a splitting for a magnetic field along a [100] direction and no effect for a [110] orientation, which is expected for a Γ_5^- line as discussed in Ref. 8. The additional rather weak line at 7.136 eV in CsBr (Fig. 10) is also assigned to a Γ_5^- exciton, though no measurements in magnetic fields are done up to now.

The second rather strong absorption at 8.449 eV in NaCl (Fig. 11) is assigned to a transition from the lower valence band (Γ_6^- symmetry) to the lowest conduction band (Γ_6^+). The much larger splitting in three-photon absorption (0.44 eV) as compared to one-photon absorption (0.16 eV) can be understood, if one remembers the fact that the three-photon resonances are taken at k_{max} on the upper polariton branches. The upper polariton branch of the lower resonance (Γ_8^- valence band) is pushed down by the close-lying strong resonance due to the Γ_6^- valence band.

For RbI and CsI we have done a detailed study of the polariton structure. In Fig. 12 we present resonances on the upper polariton branch and the longitudinal exciton branch of RbI for different k values. The relevant k configurations are indicated. The fit of a two-oscillator dispersion formula to the experimental results is shown in Fig. 13. We proceed as described for KI in Ref. 7:

$$\frac{\hbar^2c^2k^2}{E^2}=\epsilon_b\frac{E_{L1}^2-E^2}{E_{T1}^2-E^2}\frac{E_{L2}^2-E^2}{E_{T2}^2-E^2}\,. \tag{9}$$

We get for the fit parameters to the dispersion formu-

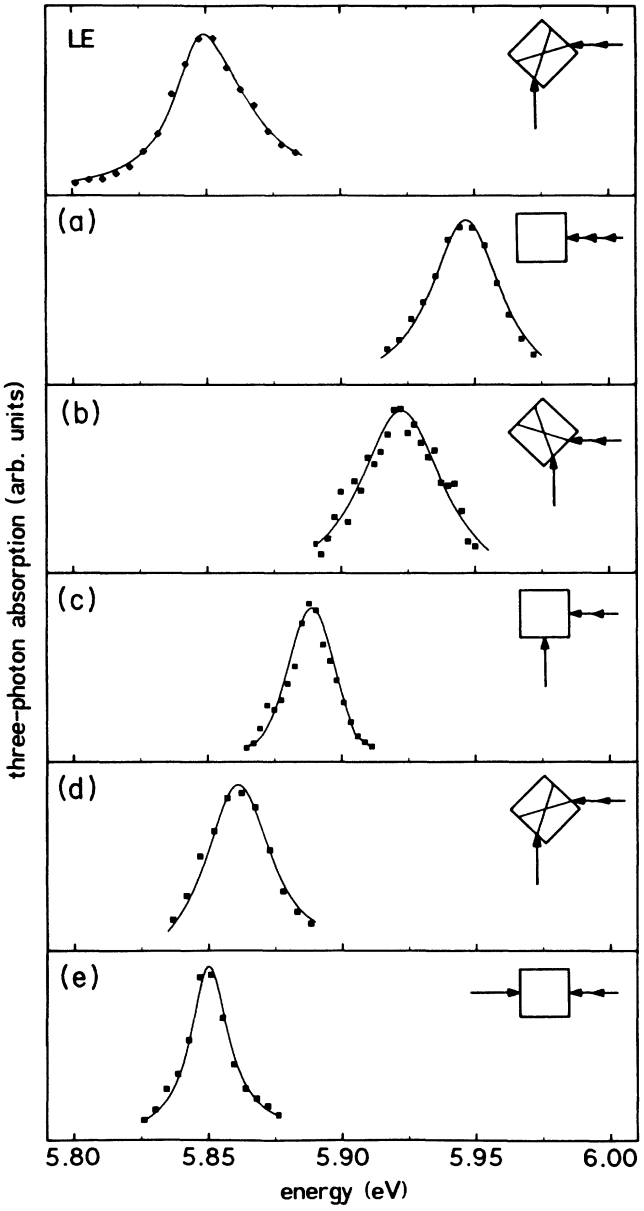

FIG. 12. Three-photon spectra of RbI at 1.5 K for k configurations as indicated. For the excitation of the LE all polarizations are in the plane of k vectors. The resonances (a)–(e) on the upper polariton branch are measured with polarizations perpendicular to the plane of k vectors.

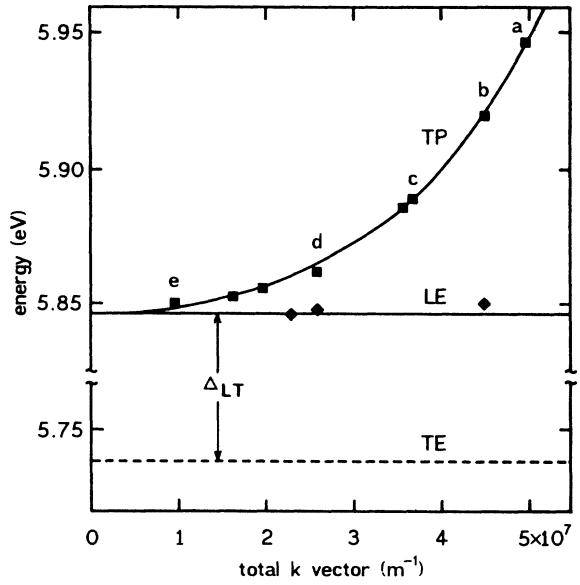

FIG. 13. Energy of the upper polariton (TP) and LE of RbI as function of total k vector. Solid and dashed lines are a fit of the experimental results by a two-oscillator model. Resonances marked (a)–(e) are shown in Fig. 12.

TABLE III. Fit parameters of polariton structure of CsI. The energy values of the oscillators 5 and 6 are calculated from data and Rodney (Ref. 24).

i	E_{Ti}	E_{Li}	Δ_{LTi}
1	5.826 eV±10 meV	5.864 eV±1 meV	38±10 meV
2	5.913 eV±3 meV	5.932 eV±1 meV	19±3 meV
3	5.988 eV±3 meV	6.016 eV±1 meV	28±3 meV
4	6.3 eV	6.5175 eV	217.5 meV
5	6.848 eV	7.2515 eV	403.5 meV
6	8.455 eV	11.181 eV	2.726 eV

la[22] [Eq. (9)] the following values: $E_{T1}=5.738$ eV, $E_{L1}=5.846$ eV, $E_{T2}=6.47$ eV, $E_{L2}=7.28$ eV, and $\epsilon_b=2.04$. From our fit we get a longitudinal-transverse splitting of $\Delta_{LT}=108$ meV which agrees quite well with recent one-photon results of Itoh and Hashimoto.[23] In CsI the polariton structure is much more complicated, since there are three close-lying resonances. In Fig. 14 we present a fit of our data to a six-oscillator dispersion formula:

$$\frac{\hbar^2c^2k^2}{E^2}=\epsilon_b\prod_{i=1}^{6}\frac{E_{Li}^2-E^2}{E_{Ti}^2-E^2}\ . \tag{10}$$

The fit parameters are given in Table III. $\epsilon_b=1.42$ is determined by the refractive index in the visible and the

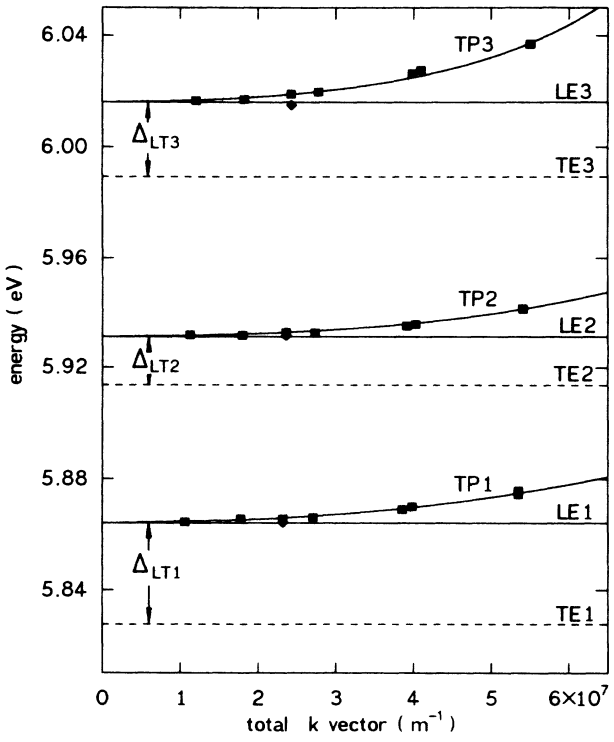

FIG. 14. Energy of upper polaritons (TP1–TP3) and longitudinal excitons (LE1–LE3) of CsI as function of total k vector. Solid and dashed lines are a fit of the experimental results by a six-oscillator model.

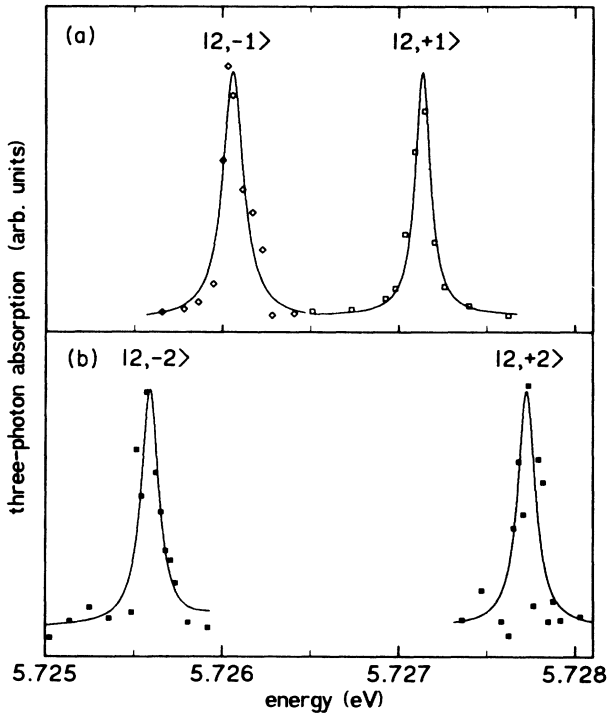

FIG. 15. Paraexciton in RbI split into four components in a magnetic field of 7 T. (a) The $M=\pm1$ components are measured in Faraday configuration with circularly polarized light of negative and positive helicity, respectively. (b) The $M=\pm2$ components are measured in Voigt configuration with linearly polarized light.

energies of the oscillators. For the lower polariton branch there exist one-photon data by Itoh and Hashimoto[23] which agree quite well with our polariton dispersion.

In the following we present three-photon magnetoabsorption measurements of RbI. As shown by Beerwerth and Fröhlich[9] for KI the paraexciton is seen in TPS if one applies high magnetic fields. In Fig. 15 we present measurements in Faraday and Voigt configuration. The $M=\pm1,\pm2$ components of the $F=2$ (Γ_3^-,Γ_5^-) paraexciton are clearly resolved. The magnetic field dependence is shown in Fig. 16. From these data one gets the g value of the paraexciton and its energy with high accuracy: $g_P=\frac{1}{4}(3g_v+g_c)=1.33\pm0.05$, $E_P=5.7266$ eV$\pm$0.2 meV. With the use of Eqs. (4) and (5) from Sec. II we get for $\varepsilon_{ex}=0.15\pm0.05$ meV. In order to determine the g values of the conduction band (g_c) and the valence band (g_v) separately one needs the g value of the orthoexciton [$g_o=\frac{1}{4}(5g_v-g_c)$]. Because of the rather large linewidth of the orthoexciton ($\sim$22 meV) there is no chance to observe a clear splitting of the $F=1$ (Γ_4^-) polariton into its components $M=\pm1$. These resonances are measured with two counterpropagating beams of different helicity. In order to avoid uncertainties due to backlash of the dye laser setting both components are measured in the same run by changing at each wavelength setting the helicity of both laser beams. From a computer fit of the $M=\pm1$ components we derive $g_0=0.95\pm0.20$. From g_p and g_o one gets $g_c=1.9\pm0.3$ and $g_v=1.1\pm0.1$. In a tight-binding model one would expect $g_c=2$ and $g_v=1.33$. Similar results were found in KI (Refs. 9 and 25) ($g_p=1.35\pm0.05$, $g_o=0.8\pm0.2$). The experimental values are given in Table IV.

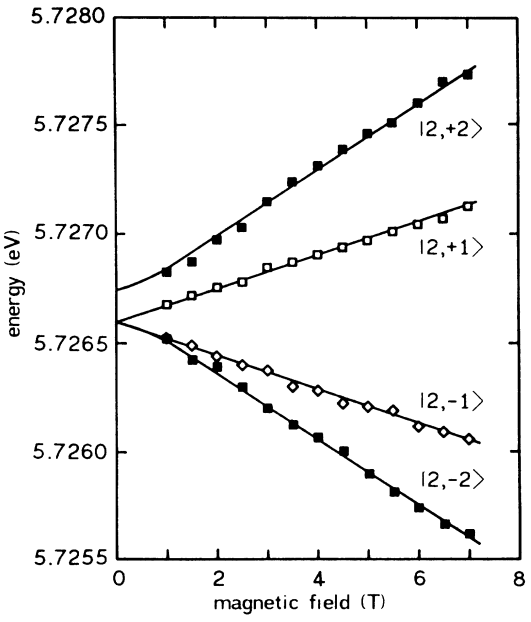

FIG. 16. Field dependent splitting of the $F=2$ paraexciton in RbI. Solid lines represent a least-squares fit with parameters given in the text.

TABLE IV. Experimental results for KI and RbI; abbreviations as defined in the text.

	KI	RbI
E_P	5.8279 eV$\pm$0.1 meV	5.7266 eV$\pm$0.2 meV
E_T	5.836 eV$\pm$3 meV	5.738 eV$\pm$3 meV
E_L	5.946 eV$\pm$1 meV	5.846 eV$\pm$1 meV
Δ_{LT}	110$\pm$3 meV	108$\pm$3 meV
Δ_{ex}	12$\pm$4 meV	17$\pm$4 meV
ε_{ex}	0.1$\pm$0.05 meV	0.15$\pm$0.05 meV
g_o	0.8$\pm$0.2	0.95$\pm$0.20
g_p	1.35$\pm$0.05	1.33$\pm$0.05

Another interesting parameter is the exchange energy which can be determined with the use of Eq. (1). We get for RbI $\Delta_{ex}=17\pm4$ meV which is again close to the value of KI (Refs. 8 and 23) (12$\pm$4 meV). Our values are smaller than recent data of Itoh[26] [Δ_{ex}(RbI)=26 meV, Δ_{ex}(KI)=20 meV]. Petroff *et al.*[27] and van Khiem and Nouailhat[28] get values for Δ_{ex}(KI) which are about a factor of 3 larger than ours. They derive their values from phonon-induced sidebands of the triplet exciton. Though there are certainly difficulties to determine the energy of the paraexciton E_P and Δ_{ex} with high accuracy from one-photon data, there might be a physical reason for the rather large discrepancies between the one- and three-photon results. As discussed by O'Connel-Bronin[29] for NaI the exciton dispersion should be taken into account to analyze the one-photon data. This point is discussed in detail by Fishman[30] and Uihlein and Feierabend.[31] In the analysis of our three-photon data, however, the exciton dispersion can probably be neglected because of the rather small total k vector which is determined by the refractive index of the laser photons in the visible spectral region [E(laser)$=\frac{1}{3}E_P$].

It would certainly be of great interest to look for paraexcitons in alkali bromides and chlorides. From the ratio of the integrated intensities of the spin-orbit doublet Onodera and Toyozawa[17] get rather large values for the exchange energy [Δ_{ex}(NaBr)=370 meV, Δ_{ex}(KBr)=260 meV, Δ_{ex}(RbBr)=160 meV, and Δ_{ex}(KCl)=53 meV].

The most interesting case for a further theoretical analysis is certainly CsI. As discussed in Sec. II there are 24 exciton states if one considers the transitions from the Γ_8^- valence band to the Γ_6^+ and Γ_8^+ conduction bands. In addition to the three Γ_4^- excitons (nine states), which are already known from one-photon absorption, we have seen two Γ_5^- excitons and one Γ_3^- exciton (eight states) in three-photon spectroscopy. From a theoretical analysis taking into account Coulomb interaction one should be able to predict the energies of the remaining excitons of Γ_1^-, Γ_2^-, Γ_3^-, and Γ_5^- symmetry (seven states), their g values, and values for the exchange energy.

From the relative oscillator strength of the different exciton lines gained by TPS one should not draw any conclusions, because these lines are detected by excitation spectroscopy, rather than by direct absorption. The resonance energies and the linewidth of the exciton lines are reliable if one assumes that the luminescence efficiency

does not change within each exciton line. TPS is specially suited to study the linewidth of the different excitons and their temperature dependence, since the spectra are taken in bulk material. The one-photon data, which are taken on evaporated films exhibit a larger linewidth, which might be due to strain and surface effects. For first results we refer to a recent publication by Beerwerth, Fröhlich, and Leinweber.[32]

[1]Ch. Uihlein, D. Fröhlich, and R. Kenklies, Phys. Rev. B **23**, 2731 (1981).

[2]H. W. Hölscher, A. Nöthe, and Ch. Uihlein, Phys. Rev. B **31**, 2379 (1985).

[3]Ch. Neumann and A. Nöthe, Europhys. Lett. **4**, 351 (1987).

[4]Ch. Neumann, A. Nöthe, and N. O. Lipari, Phys. Rev. B **37**, 922 (1988).

[5]D. Fröhlich, E. Mohler, and P. Wiesner, Phys. Rev. Lett. **26**, 554 (1971); D. Fröhlich, E. Mohler, and Ch. Uihlein, Phys. Status Solidi B **55**, 175 (1973).

[6]D. Fröhlich, K. Reimann, and P. Koidl, Phys. Status Solidi B **114**, 553 (1983).

[7]F. Beerwerth and D. Fröhlich, Phys. Rev. Lett. **55**, 2603 (1985).

[8]F. Beerwerth and D. Fröhlich, Phys. Rev. Lett. **57**, 1344 (1986).

[9]F. Beerwerth and D. Fröhlich, Phys. Rev. B **36**, 6239 (1987).

[10]R. Hilsch and R. W. Pohl, Z. Phys. **59**, 812 (1930).

[11]W. Martienssen, J. Phys. Chem. Solids **2**, 257 (1957).

[12]K. Teegarden and G. Baldini, Phys. Rev. **155**, 896 (1967).

[13]R. S. Knox, *Theory of Excitons* in *Solid State Physics,* edited by H. Ehrenreich, F. Seitz, and D. Turnbull (Academic, New York, 1963), Suppl. 5, p. 59.

[14]B. Kunz, Phys. Rev. **175**, 1147 (1968); J. Chem. Solids **31**, 265 (1970).

[15]Y. Onodera, J. Phys. Soc. Jpn. **25**, 469 (1968).

[16]G. F. Koster, J. O. Dimmock, R. G. Wheeler, and H. Statz, *Properties of the Thirty-Two Point Groups* (MIT Press, Cambridge, MA, 1963).

[17]Y. Onodera and Y. Toyozawa, J. Phys. Soc. Jpn. **22**, 833 (1967).

[18]H. Iwamoto and R. Onaka, J. Phys. Soc. Jpn. **52**, 3992 (1983).

[19]K. Cho, S. Suga, W. Dreybrodt, and F. Willmann, Phys. Rev. B **11**, 1512 (1975); **12**, 1608 (1975).

[20]K. Maier, J. Cryst. Growth **6**, 111 (1969).

[21]N. Itoh, Ad. Phys. **31**, 491 (1982).

[22]T. Kurosawa, J. Phys. Soc. Jpn. **16**, 1298 (1961).

[23]M. Itoh and S. Hashimoto, J. Phys. Soc. Jpn. **55**, 399 (1986); **55**, 4513 (1986).

[24]W. S. Rodney, J. Opt. Soc. Am. **45**, 987 (1955).

[25]F. Beerwerth and D. Fröhlich, J. Lumin. **40&41**, 435 (1988).

[26]M. Itoh, Phys. Rev. B **35**, 7652 (1987).

[27]Y. Petroff, R. Pinchaux, C. Chekroun, M. Balkanski, and H. Kamimura, Phys. Rev. Lett. **27**, 1377 (1971).

[28]T. van Khiem and A. Nouailhat, Solid State Commun. **37**, 587 (1981).

[29]A. A. O'Connel-Bronin, Phys. Status Solidi B **129**, 675 (1985).

[30]G. Fishman, Solid State Commun. **27**, 1097 (1978).

[31]Ch. Uihlein and S. Feierabend, Phys. Status Solidi B **94**, 153 (1979).

[32]F. Beerwerth, D. Fröhlich, and V. Leinweber, Phys. Status Solidi B **145**, 95 (1988); J. Lumin. **40&41**, 477 (1988).